ASSESSING VACCINATION EFFICACY IN HIGH-TREATMENT SATURATION FOR MENINGITIS CONTROL

Received
August 10, 2024

Revised
October 02, 2024

Accepted
October 14, 2024

*Mutairu K. KOLAWOLE[1], Amos O. POPOOLA[2], Adebiyi A. ADEGOKE[1]
[1,2]Faculty of Basic and Applied Sciences, Department of Mathematical Sciences, Osun State University, Osogbo, Nigeria
[3]Faculty of Basic and Medical Sciences, Department of Anatomy, Osun State University, Osogbo, Nigeria
Email: mutairu.kolawole@uniosun.edu.ng

Abstract: The study investigates the effectiveness of vaccination to keep meningitis in check, especially in conditions of high treatment saturation and limited resources. The numerical solution of this model is obtained through the homotopy perturbation method. In this work, we examine how vaccination and treatment are interrelated, but above all, with the basic reproduction number R_0, an important tool that identifies the size of the spread of meningitis. The study performs analyses of local and global stability for disease-free and endemic equilibrium points, providing insight into when and how meningitis can be eradicated or persist within a population. Furthermore, sensitivity analysis provides further light on which parameters have more influence on the disease transmission, thus providing an understanding of what factors would most ensure the control measures are successfully executed. In this paper, we have incorporated vaccination and treatment strategies into the model in order to assess the combined effect of the two methods in reducing the spread of meningitis and the best approaches towards disease control. In this dynamics, we apply the homotopy perturbation method for a comprehensive view of how vaccination and treatment can mitigate the burden of meningitis. These findings realize key lessons for the improvement of meningitis control strategies, particularly in remote settings, and hence contribute to the wider debate on infectious disease control. This in turn shows a way toward better control by demonstrating how a vaccination and treatment strategy that is strategically balanced can reduce the overall burden of the disease over time.

Keywords: *Meningitis, High treatment saturation, Vaccination, Stability analysis, Homotopy perturbation method*

1. INTRODUCTION

Meningitis, a severe and potentially fatal infection of the protective membranes surrounding the brain and spinal cord, it poses a persistent public health challenge worldwide. To combat the devastating impact of this disease, various control measures have been employed, with vaccination playing a pivotal role [1]. Vaccination programs have been successful in reducing the burden of meningitis in many regions, but the effectiveness of these programs can vary significantly depending on the local context and the availability of treatment resources [2]. Undertaken a comprehensive examination of the efficacy of vaccination as a key component of meningitis control in settings where treatment resources are already saturated. We intentionally incorporate a saturated treatment function into our analysis to capture the refined association between vaccination and treatment under conditions of limited resources and heightened disease prevalence [4]. Meningitis is an inflammation of the protective membranes surrounding the brain and spinal cord, which has left a long and troubling mark on human history [3].

This disease, often caused by bacteria or viruses, can strike swiftly, leading to severe illness, long-term disability, and even death [5]. Throughout the years, mankind has sought various measures to combat its devastating effects, and vaccination stands as a pivotal intervention in this ongoing battle [8]. The control measures typically encompass a range of strategies, including early diagnosis, timely treatment with antibiotics, surveillance, and public health interventions and these strategies have undoubtedly saved lives and prevented outbreaks, the challenge arises when disease incidence surpasses the available treatment capacity [6,7]. In such high-treatment saturation conditions, the role of vaccination becomes particularly critical, as it can reduce the overall disease burden and mitigate the strain on already overwhelmed healthcare systems [9].The a pressing need to better understand the dynamics of vaccination in scenarios where treatment

resources are stretched to their limits [10, 11]. By systematically assessing vaccination efficacy in high-treatment saturation conditions, we aim to provide insights that can inform more effective and efficient Meningitis control strategies [12]. We recognize that these conditions may be more prevalent in resource-limited or conflict-affected regions, making our research particularly relevant to those regions where healthcare infrastructure is already strained [13]. Various pathogens, including Neisseria meningitidis, Streptococcus pneumoniae, and Haemophilus influenzae [14,15]. The transmission modes vary from person to person, with respiratory droplets and close contact serving as common routes. Once infection occurs, its consequences can be profound, encompassing neurological damage, hearing loss, cognitive impairments, and a significant mortality rate [16]. The efforts to control meningitis have historically relied on a combination of strategies, such as prompt diagnosis, antibiotic treatment, and public health interventions [17]. However, these control measures face challenges when disease incidence exceeds the healthcare system's treatment capacity in [18]. Under such conditions, vaccination emerges as a key tool for reducing disease burden and preventing outbreaks [19]. Scrutinizes the effectiveness of vaccination in scenarios where treatment resources are saturated. By incorporating a saturated treatment function, we aim to shed light on the nuanced interplay between vaccination and treatment under these challenging conditions [20-23]. This research contributes to the broader discourse on infectious disease control and strives to offer insights that can enhance the efficiency and efficacy of meningitis control strategies.

The spectrum of meningitis cases includes bacterial, viral, and fungal etiologies, with bacterial meningitis often being the most fatal [24]. Despite global advancements in healthcare and medicine, meningitis remains a persistent threat, particularly in resource-limited settings [25, 26, 35]. One of the most effective strategies for reducing the burden of meningitis is vaccination, which has been widely deployed in various regions with mixed outcomes [27]. Bacterial meningitis, caused by pathogens such as (Neisseria meningitidis, Streptococcus pneumoniae, and Haemophilus influenzae), remains the most severe form of the disease, often leading to long-term disability or death if not promptly treated [28, 30]. Viral meningitis, while generally less severe, also contributes significantly to the overall disease burden, particularly in low- and middle-income countries [29, 31]. The transmission of meningitis typically occurs through respiratory droplets or close contact, making it a highly contagious and dangerous pathogen in densely populated areas or during outbreaks [33, 34].

Local and global stability analyses play a pivotal role in understanding the transmission dynamics of meningitis. These mathematical approaches help determine whether the disease will persist or be eradicated under varying conditions [32]. This focuses on small deviations from the disease-free equilibrium, assessing whether minor disturbances, such as isolated cases of infection, will lead to sustained outbreaks or if the disease will naturally die out [36]. If the disease-free equilibrium is locally stable, minor increases in infection will not result in widespread transmission, signifying that control measures, such as vaccination and treatment, are effective in maintaining low disease prevalence. Global stability analysis examines the system's behavior over a wider range of conditions, determining whether the population will eventually return to a disease-free state regardless of initial infection levels [37]. A globally stable disease-free equilibrium indicates that meningitis can be eradicated in the long term, even in the presence of high initial infection rates [38]. By identifying conditions for both local and global stability, these analyses provide crucial insights into the effectiveness of control measures [41]. If the endemic equilibrium is unstable, it signals a need for stronger interventions, such as improved vaccination coverage or enhanced treatment strategies, to curb meningitis transmission and prevent outbreaks.

The control of meningitis has historically relied on a combination of strategies, including early diagnosis, antibiotic treatment, surveillance, and public health interventions such as vaccination. Vaccination, in particular, has been instrumental in reducing the global burden of meningitis [39]. The lack of vaccination and proper treatment for meningitis, especially in rural settings, exacerbates the disease's spread, overwhelming healthcare systems. The critical role of vaccination in reducing disease burden, particularly when treatment resources are saturated is required [40]. By employing the homotopy perturbation method, we utilize the importance of optimizing both vaccination and treatment strategies to effectively control meningitis and prevent its devastating impact.

2. Methods

2.0 Model formulation

We consider a mathematical model of linear differential equations for determining the spread of meningitis between a groups of population. For a disease modification factor, the population is subdivided into

different epidemiological classes: Susceptible $S(t)$, vaccinated $V(t)$, Exposed $E(t)$, Infected, and recovered $R(t)$ individuals. Recruitment into the susceptible population and the transmission probability is deduced as π and β. An exposed individual to meningitis spread can be developed vastly to infected population at σ. Meningitis spread can be controlled through treatment when early discovered at rate of τ, the effect of low immunity level in subpopulation which may or may not be of importance as naturally every being is subjected to death by nature is denoted by μ. However, if the treatment is effective on the individuals and the level at which is this brings about the recovery rate at γ_e for exposed and γ_i infected individuals. .Individuals in the susceptible class has an immunity rate of κ after recovery at a rate κ. The vaccination efficacy ε will be applicable to the population of infected individuals migrating to the recovered population. The disease-induced death rate and treatment inhibitor are respectively given as δ and α. The above illustration can be represented in a Schematic diagram and a system of nonlinear differential equations in Figure 1 and Equation 1 respectively.

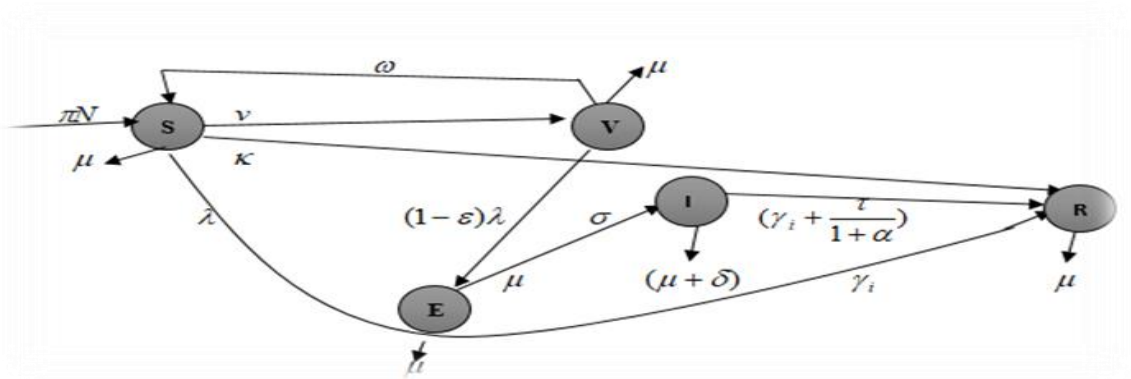

Fig.1: Schematic flow of the model formulation

$$\left.\begin{aligned}
\frac{dS}{dt} &= \pi N + \omega V + \kappa R - \lambda S - (\nu + \mu)S \\
\frac{dV}{dt} &= \nu S - (1-\varepsilon)\lambda V - (\omega + \mu)V \\
\frac{dE}{dt} &= \lambda S + (1-\varepsilon)\lambda V - (\sigma + \mu + \gamma_c)E \\
\frac{dI}{dt} &= \sigma E - (\gamma_i + \mu + \delta)I - \frac{\tau I}{1+\alpha I} \\
\frac{dR}{dt} &= \gamma_c E + \left(\gamma_i + \frac{\tau I}{1+\alpha I}\right)I - (\kappa + \mu)R
\end{aligned}\right\} \qquad (1)$$

Subject to the following initial conditions

$$\text{Consider } \lambda = \frac{\beta(\eta C + I)}{N} \text{ and } S(0) = s_0, V(0) = v_0, E(0) = e_0, I(0) = i_0, R(0) = r_0 \geq 0 \qquad (2)$$

Analysis of the model

2.1. Existence and uniqueness of model solution

The system (1), which describes an epidemic disease within a human population, should have parameters that are nonnegative. To ensure that the system of differential equations in (1) is both mathematically and epidemiologically well-posed, it is essential to demonstrate that the state variables in the model are nonnegative. System (1) is well-posed when the system starts. Non-negative initial conditions

$S(0)=s_0, V(0)=v_0, E(0)=e_0, I(0)=i_0, R(0);$

In that case, the solutions of system (1) will persist in being nonnegative throughout their evolution, $t>0$ and that these positive solutions are bounded. We thus apply the following theorems.

Theorem 1

Proof:

Let $\lambda_0 \in [0,1]$ then $p(\lambda_0)=\lambda_0 x+(1-\lambda_0)y$ for any $\lambda_0 \in [0,1]$,

$$\|p(\lambda)-p(\lambda_0)\| = \|(\lambda-\lambda_0)x+(\lambda-\lambda_0)y\| \leq |\lambda-\lambda_0|(\|x\|+\|y\|) \quad (3)$$

If $\varepsilon>0$ is given , let $\delta=\frac{\varepsilon}{\|x\|+\|y\|}$ .If $|\lambda-\lambda_0|<\delta$, then the $\|p(\lambda)-p(\lambda_0)\|<\varepsilon$. Therefore, p is continuous at λ_0. The interval of continuity is on [0. 1] as λ_0 is an arbitrary point.. Let X be a linear space over $\Re$. If x,y are distinct points of X, the set $\lambda x+(1-\lambda)y$ lies in $0\leq\lambda\leq 1$

Hence, the solutions of system (1) are bounded if we consider the total population

$N(t)=\mathrm{S(t)+V(t)+E(t)+I(t)+R(t)}$

The system (1), which describes an epidemic disease within a human population, should have parameters that are nonnegative. To ensure that the system of differential equations in (1) is both mathematically and epidemiologically well-posed, it is essential to demonstrate that the state variables in the model are nonnegative. System (1) is well-posed. Consider a system starting with nonnegative initial conditions

$S(0)=s_0, V(0)=v_0, E(0)=e_0, I(0)=i_0, R(0);$

In that case, the solutions of system (1) will persist in being nonnegative throughout their evolution, $t>0$ and that these positive solutions are bounded. We thus apply the following theorem.

The variation in the total population concerning time is given by:

Let (x,y) be distinct points of normed linear space $(X,\|\cdot\cdot\|)$ over $\Re$. Then the map of $p:[0,1]\subseteq\Re\rightarrow(X,\|\cdot\cdot\|)$ such that $p(\lambda)=\lambda x+(1-\lambda)y$ is continuous on [0,1].

$$\frac{dN(t)}{dt}=\frac{d}{dt}\left(\mathrm{S(t)+V(t)+E(t)+I(t)+R(t)}\right) \quad (4)$$

$$\frac{dN(t)}{dt}=\pi N-\mu(S+V+E+I+R)-\delta I \qquad \Rightarrow \frac{dN(t)}{dt}\leq \pi N-\mu N \text{ at } \delta=0$$

Thus, it is obtained that

$$\frac{dN(t)}{dt}+\mu N\leq \pi N,\ N(t)e^{\mu t}=\frac{\pi N}{\mu}e^{\mu t}+C \quad \text{where } C \text{ is a constant of integration} \quad (5)$$

Initially when $t=0$,

$N(0)=\frac{\pi N}{\mu}+ce^{-\mu(0)}$, this yields

$$c=N(0)-\frac{\pi N}{\mu} \quad (6)$$

Thus, substituting (6) into (5) as time progressively increases yields:

$$\lim_{t\to\infty} N(t) \le \lim_{t\to\infty}\left[\frac{\pi N}{\mu}+\left(N(0)-\frac{\pi N}{\mu}\right)e^{-\mu t}\right]=\frac{\pi N}{\mu} \tag{7}$$

If so $N(0)\le\frac{\pi N}{\mu}$ at $t=0$, then $N(t)\le\frac{\pi N}{\mu}$ when $t=0$. This is a positive invariant set under the flow described by (2) so that no solution path leaves through any boundary $\Re_+^5$. Hence, it is sufficient to consider the dynamics of the model in the domain $\Re_+^5$. In this deduction it is said that the model solution is bounded from above with epidemiology representation of a physical problem. This shows that the total population $N(t)$, and the subpopulation $S(t),E(t),I(t),R(t)$. Hence, its applicability to study physical systems is feasible.

This shows that the total population $N(t)$, and the subpopulation $S(t),E(t),I(t),T(t),R(t)$ of the model are bounded. Hence, its applicability to study physical systems is feasible.

2.2. Positivity and boundedness of model solution

Theorem 2

*G*iven that $X=x_0$ is a bounded region on $x\in[0,1]$ defined by

$$L(x,y)=\left(\sum_{i=1}^{n}\left|x_i\right|^{\Omega}\right)^{\frac{1}{\Omega}} \qquad \Omega\ge 1 \tag{8}$$

X with the metric is called ξ_n^{Ω} space. If $\sum^{\infty}|x|^{\Omega}<\infty$ or absolutely convergent and $L(x,y)=\left(\sum_{i=1}^{\infty}\left|x_i-y_i\right|^{\Omega}\right)^{\frac{1}{\Omega}}$, then X with this metric is called an ξ^{Ω} space.

Proof:

It can be checked that for each n:

$$0\le x_1^2+x_2^2+x_3^2+...+x_n^2\le\left(|x_1|+|x_2|+|x_3|+...+|x_n|\right)^2 \tag{9}$$

This will result to;

$$x_1^2+x_2^2\le\left(|x_1|+|x_2|\right)^2 \tag{10}$$

Therefore,

$$0\le\left(x_1^2+x_2^2+x_3^2+...+x_n^2\right)^{\frac{1}{2}}\le\left|x_1\right|^2+\left|x_2\right|^2+\left|x_3\right|^2+...+\left|x_n\right|^2,$$

If $\sum_{n=1}^{\infty}|x_n|$ converges, that is $\sum_{n=1}^{\infty}|x_n|$ is absolutely convergent, then

$$0\le\left(x_1^2+x_2^2+x_3^2+...+x_n^2\right)^{\frac{1}{2}}\le\left|x_1\right|^2+\left|x_2\right|^2+\left|x_3\right|^2+...+\left|x_n\right|^2=\sum_{n=1}^{\infty}|x_n|<\infty \tag{11}$$

Therefore,

$$0\le x_n=x_1^2+x_2^2+x_3^2+...+x_n^2\le\left[\sum_{n=1}^{\infty}|x_n|\right]<\infty \tag{12}$$

it therefore converges. Thus $\sum_{n=1}^{\infty}x_n$ converges absolutely, i. E if $x_n\in\xi^1$, then $x_n\in\xi^2$ where $\xi^1\le\xi^2$. In case of ξ^1 denote the set of all variables of x_n of real numbers such that $\sum_{n=1}^{\infty}x_n$ is convergent

absolutely. i.e $\sum_{n=1}^{\infty}|x_n|<\infty$ and ξ^2 denote the set of all variables x_n of real numbers such that $\sum_{n=1}^{\infty}x_n^2<\infty$ converges. From the proceeding $x_n\in\xi^1\Leftrightarrow x_n\in\xi^2$ i.e. $\xi^1\subseteq\xi^2$. Further, if $x_n=\frac{1}{n^{\frac{3}{4}}}$, then $\sum_{n=1}^{\infty}|x_n|$ diverges and thus $x_n\notin\xi^1$. But $\sum_{n=1}^{\infty}x_n^2\le\sum_{n=1}^{\infty}\frac{1}{n^{\frac{3}{4}}}$ converges, implying that $x_n\in\xi^2$. We conclude that $\xi^1\subseteq\xi^2$ and thus $\xi^1\neq\xi^2$. If (x_n,y_n) are sets of real numbers, then;

$$\sum_{n=1}^{\infty}(x_i-y_i)^2\le\sum_{n=1}^{\infty}x_i^{\,2}+\sum_{n=1}^{\infty}y_i^{\,2}+2\left[\sum_{n=1}^{\infty}x_i^{\,2}\right]^{\frac{1}{2}}\left[\sum_{n=1}^{\infty}y_i^{\,2}\right]^{\frac{1}{2}} \tag{13}$$

Therefore if $\sum_{n=1}^{\infty}x_i^{\,2}<\infty$ and $\sum_{n=1}^{\infty}y_i^{\,2}<\infty$ then $\sum_{n=1}^{\infty}(x_i-y_i)^2<\infty$ for all n. The monotone increasing sequence $\left[\sum_{n=1}^{\infty}(x_i-y_i)^2\right]$ is then bounded above and hence converges i.e. $\sum_{n=1}^{\infty}(x_i-y_i)^2<\infty$. Thus $(x_i-y_i)^2\in\xi^2$ if $(x_n,y_n)\in\xi^2$.

Given that the $S(0)=s_0>0,V(0)=v_0>0,E(0)=e_0>0,I(0)=i_0>0,R(0)=r_0>0$, and $t>0$, then the solutions $S(t),V(t),E(t),I(t),R(t)$ of the system (1) will always be nonnegative.

Let: $\Pi=\left\{(S(t),V(t),E(t),I(t),R(t))\in\Re_+^5:N(t)\le\frac{\pi N}{\mu}\right\}$ (14)

and $f_i,i=1,2\ldots.5$ where f is a constant.

$$\begin{aligned}
f_1&=\pi N+\omega V+\kappa R-\lambda S-(\nu+\mu)S\\
f_2&=\nu S-(1-\varepsilon)\lambda V-(\omega+\mu)V\\
f_3&=\lambda S+(1-\varepsilon)\lambda V-(\sigma+\mu+\gamma_e)E\\
f_4&=\sigma E-(\gamma_i+\mu+\delta)I-\frac{\tau I}{1+\alpha I}\\
f_5&=\gamma_c E+\left(\gamma_i+\frac{\tau I}{1+\alpha I}\right)I-(\kappa+\mu)R
\end{aligned} \tag{15}$$

Then,

$$\left.\begin{array}{l}
\left|\frac{df_1}{dS}\right| = \left|\lambda + (\nu + \mu)\right| < \infty, \left|\frac{df_1}{dV}\right| = \left|\omega\right| < \infty, \left|\frac{df_1}{dE}\right| = \left|0\right| < \infty, \left|\frac{df_1}{dI}\right| = \left|0\right| < \infty, \left|\frac{df_1}{dR}\right| = \left|\kappa\right| < \infty \\
\left|\frac{df_2}{dS}\right| = \left|\nu\right| < \infty, \left|\frac{df_2}{dV}\right| = \left|(1-\varepsilon)\lambda\right| < \infty, \left|\frac{df_2}{dE}\right| = \left|0\right| < \infty, \left|\frac{df_2}{dI}\right| = \left|0\right| < \infty, \left|\frac{df_2}{dR}\right| = \left|0\right| < \infty \\
\left|\frac{df_3}{dS}\right| = \left|0\right| < \infty, \left|\frac{df_3}{dV}\right| = \left|(1-\varepsilon)\lambda\right| < \infty, \left|\frac{df_3}{dE}\right| = \left|(\sigma + \mu + \gamma_e)\right| < \infty, \left|\frac{df_3}{dI}\right| = \left|0\right| < \infty, \left|\frac{df_3}{dR}\right| = \left|0\right| < \infty \\
\left|\frac{df_4}{dS}\right| = \left|0\right| < \infty, \left|\frac{df_4}{dV}\right| = \left|0\right| < \infty, \left|\frac{df_4}{dE}\right| = \left|\sigma\right| < \infty, \left|\frac{df_4}{dI}\right| = \left|(\gamma_i + \mu + \delta) + \frac{\tau}{1+\alpha}\right| < \infty, \left|\frac{df_4}{dR}\right| = \left|0\right| < \infty \\
\left|\frac{df_5}{dS}\right| = \left|0\right| < \infty, \left|\frac{df_5}{dV}\right| = \left|0\right| < \infty, \left|\frac{df_5}{dE}\right| = \left|\gamma_e\right| < \infty, \left|\frac{df_5}{dI}\right| = \left|\frac{\tau}{1+\alpha}\right| < \infty, \left|\frac{df_5}{dR}\right| = \left|(\kappa + \mu)\right| < \infty
\end{array}\right\} \quad (16)$$

Equation (15) demonstrates the presence of system (1) within the positive quadrant, leading it to ultimately enter and persist in the attracting subset Π. Consequently, the set comprises both the local and global attractors of system (1). As a result, the set is characterized as compact, positively invariant, and attractively influential with respect to the system. The solution of the model is bounded, well-posed and epidemiologically represented.

2.3 Meningitis-Non-Infected Equilibrium State

The meningitis- non-infected equilibrium state represents a scenario in which the system is entirely free from meningococcal disease. Consequently, when the number of infected individuals (I), it follows that the numbers of exposed (E) and recovered (R), i.e. When there is no outbreak of meningitis in the set of population considered the disease classes such as E and I are subjected to $I = E = 0$. In this context, the solution for the meningitis-free equilibrium point can be derived as follows:

$\frac{dS}{dt} = \frac{dV}{dt} = \frac{dE}{dt} = \frac{dI}{dt} = \frac{dR}{dt} = 0$ where $\frac{dN}{dt} = 0$. Hence,

(17)

$$\begin{aligned}
&\pi N + \omega V + \kappa R - \lambda S - (\nu + \mu)S = 0 \\
&\nu S - (1-\varepsilon)\lambda V - (\omega + \mu)V = 0 \\
&\lambda S + (1-\varepsilon)\lambda V - (\sigma + \mu + \gamma_e)E = 0 \\
&\sigma E - (\gamma_i + \mu + \delta)I - \frac{\tau I}{1+\alpha I} = 0 \\
&\gamma_c E + \left(\gamma_i + \frac{\tau I}{1+\alpha I}\right)I - (\kappa + \mu)R = 0
\end{aligned} \quad (17)$$

At no outbreak of meningitis the diseases class are subjected as $t = 0$, from above the system of equation (1) results to (17) from (12),

$\gamma_c E + \left(\gamma_i + \frac{\tau I}{1+\alpha I}\right)I - (\kappa + \mu)R = 0$, if the disease population $E = I = 0$ then $R = 0$. Similarly,

$S = \frac{\pi N + \omega V}{(\lambda + \mu + \nu)}$ where $V = \frac{S}{(\varepsilon - 1)}$

Thus, the disease free equilibrium yields: $(S,V,E,I,R)=\left(S_0=\frac{\pi N(1-\varepsilon)}{((1-\varepsilon)(\lambda+\nu+\mu)+\omega)},V_0=\frac{\pi N}{((\varepsilon-1)(\lambda+\nu+\mu)+\omega)},E_0=0,I_0=0,R_0=0\right)$ (18)

2.4 Steady-State Prevalence

Meningitis prevalence on (S,V,E,I,R) at $t\neq 0$, highlighting its dynamic nature.to measure vital role on its outbreaks and protect the population. Let $E_e=(S^*,V^*,E^*,I^*,R^*)$ at steady state $I\neq 0$. Consider the system of equation in (1) the equilibrium points are:

$$S^*=\frac{(1-\varepsilon)\kappa\tau\nu^2\sqrt{(\nu+\mu)(\sigma+\gamma_e+\mu)\nu(\mu+\gamma_i+\delta)}\beta\eta(1-\varepsilon)^2[\pi\lambda+(\mu+\gamma_e+\sigma)V^*]+\varepsilon[V^*((\mu+\gamma_i+\delta)\sigma\gamma_i+\delta)]}{\mu(\omega+\mu)[(\mu+\gamma+k)(\mu+\gamma_i+\delta)+(1-\varepsilon)]}$$

$$V^*=\frac{S^*\lambda(\omega+\mu)}{\mu\beta\alpha\eta(\mu+\gamma_e+\sigma)[(\mu+\gamma+k)(\mu+\gamma_i+\delta)+(1-\varepsilon)]}$$

$$E^*=\frac{\beta\eta\tau\omega(1-\varepsilon)(\sigma+\gamma_e+\mu)S^*I^*}{\alpha\lambda\sqrt{(\omega+\nu+\mu)(\delta+\mu+\sigma)}+(\tau+\alpha)(S^*+I^*)}$$

$$I^*=\frac{(1-\varepsilon)][\pi\lambda(\tau+\alpha)+(\mu+\gamma_e+\sigma)V^*]}{[\mu^2(\omega+\mu)+(1-\varepsilon)]}-\frac{\sqrt{(\omega+\nu+\mu)(\delta+\mu+\sigma)}}{(1+\alpha I^*)^{-1}(\gamma+\mu+k)} \quad (19)$$

$$R^*=(1+\alpha I^*)^{-1}\sqrt{\frac{[(\gamma_e+\mu+k)\sigma\gamma+\delta]E^*+\pi\nu^2}{(\tau+\alpha)(\gamma_i+\mu+k)(\varepsilon+\mu+\delta)}}$$

2.5 Basic Reproduction Number

The basic reproduction number, denoted as R_0, measures the potential for new meningitis infections from a single carrier or infected individual in a population with no prior infections. To determine the system (1), we apply the next-generation method, focusing on the infectious classes E and I. This involves calculating the F and V matrices, representing the rates of new infections and transitions into and out of the infected compartment, respectively. From the equations in the system (1), we derive these matrices as follows. $R_*=\rho|G-\lambda I|$ Where $G=F\times V^{-1}$ and ρ is the spectral radius of the matrix $|G-\lambda I|$.

From the system of equation (1) it is obtained for matrix F and V :

$$F_i=\left(\frac{\partial f_i(x_i)}{\partial x_j}\right),V_i=\left(\frac{\partial \nu_i(x_i)}{\partial x_j}\right) \quad (20)$$

Such that

$$f=\begin{pmatrix}\lambda(S_0+(1-\varepsilon))\\0\end{pmatrix} \text{ And } \nu=\begin{pmatrix}(\sigma+\mu+\gamma_e)E\\-\sigma E+\left((\gamma_i+\mu+\delta)+\frac{\tau}{1+\alpha}\right)I\end{pmatrix} \quad (21)$$

Then,

$$F = \begin{pmatrix} \dfrac{\pi(\alpha+1)(1-\varepsilon)+\sqrt{\pi\eta(1-\varepsilon)\beta+(\omega\kappa+\nu+\mu)}}{\left((1-\varepsilon)^2\alpha(\lambda+\nu+\mu)+\tau\omega\right)(\sigma+\gamma_e+\mu)(\delta+\gamma_i+\mu)} & 0 \\ 0 & 0 \end{pmatrix}$$

$$V = \begin{pmatrix} (\sigma+\mu+\gamma_e) & 0 \\ -\sigma & \left((\gamma_i+\mu+\delta)+\dfrac{\tau}{1+\alpha}\right) \end{pmatrix}$$

$$V^{-1} = \begin{pmatrix} \dfrac{(1+\alpha)+\tau}{(\gamma_i+\mu+\delta)(1+\alpha)} & \dfrac{\sigma}{(\gamma_e+\mu+\sigma)(\delta+\mu+\sigma)} \\ 0 & \dfrac{1}{(\gamma_e+\mu+\sigma)} \end{pmatrix} \tag{22}$$

Thus, the R_* is obtained as

$$R_* = \frac{\pi\tau(\alpha+1)(1-\varepsilon)+\sqrt{\pi\eta(1-\varepsilon)\beta+(\omega\kappa+\nu+\mu)}}{\left((1-\varepsilon)^2\alpha(\lambda+\nu+\mu)+\tau\omega\right)(\sigma+\gamma_e+\mu)(\delta+\gamma_i+\mu)} \tag{23}$$

2.6 Asymptotic Stability of the Disease-Free State

This section examines the stability of the disease-free state for meningitis by analyzing the basic reproduction number's impact. When the reproduction number is $R_* < 1$, the disease declines, and we determine stability using a Jacobian matrix and a characteristic equation.

The disease-free equilibrium is obtained as the Jacobian matrix of the system of (1) is obtained and evaluated at the disease free-state using the linearization method

Theorem 3

The disease-free state of the model is locally Asymptotically Stable $R_* < 1$ and unstable if $R_* > 1$

Proof:

$$J_{(E_1)} = \begin{vmatrix} -(\lambda+\nu+\mu) & \omega & 0 & 0 & \kappa \\ \nu & -[(1-\varepsilon)\lambda+(\omega+\mu)] & 0 & 0 & 0 \\ \lambda & (1-\varepsilon)\lambda & -(\sigma+\gamma_e+\mu) & 0 & 0 \\ 0 & 0 & \sigma & -\left((\gamma_i+\mu+\delta)+\dfrac{\tau}{(1+\alpha)}\right) & 0 \\ 0 & 0 & \gamma_e & \left(\gamma_i+\dfrac{\tau}{(1+\alpha)}\right) & -(\mu+\kappa) \end{vmatrix} \tag{24}$$

Computing for the eigenvalues, $\left|J_{E_1}-\lambda_i I\right| = 0$

$$\begin{vmatrix} -(\beta\eta+v+\mu)-\lambda_1 & \omega & 0 & 0 & \kappa \\ v & -[(1-\varepsilon)\beta\eta+(\omega+\mu)]-\lambda_2 & 0 & 0 & 0 \\ \lambda & (1-\varepsilon)\lambda & -(\sigma+\gamma_e+\mu)-\lambda_3 & 0 & 0 \\ 0 & 0 & \sigma & -\left((\gamma_i+\mu+\delta)+\dfrac{\tau}{(1+\alpha)}\right)-\lambda_4 & 0 \\ 0 & 0 & \gamma_e & \left(\gamma_i+\dfrac{\tau}{(1+\alpha)}\right) & -(\mu+\kappa)-\lambda_5 \end{vmatrix}=0$$

as obtained:

$$\left.\begin{aligned} &\lambda_1=-(\beta\eta+v+\mu),\lambda_2=-[(1-\varepsilon)\beta\eta+(\omega+\mu)],\begin{vmatrix} -(\sigma+\gamma_e+\mu) & 0 \\ \sigma & \left((\gamma_i+\mu+\delta)+\dfrac{\tau}{(1+\alpha)}\right) \end{vmatrix},\lambda_3=-\frac{(\sigma+\gamma_e+\mu)+\tau(\gamma_i+\mu+\delta)}{(1+\alpha)^2}, \\ &\lambda_4=-\left((\gamma_i+\mu+\delta)+\frac{\tau}{(1+\alpha)}\right),\lambda_4=-(\omega+\mu) \end{aligned}\right\} \quad (25)$$

The eigenvalues are negatively invariant in the region $\Re_+^5$, hence the system of (1) is asymptotically stable.

2.7 Regional Resilience of the Persistent Equilibrium

Theorem 4

The regional resilience of the persistent equilibrium of the proposed model is locally asymptotically Stable if and unstable otherwise.

Proof:

Suppose, $S=p+S^*, V=q+V^*, E=r+E^*, I=a+I^*, R=b+R^*$

Linearizing equation (1), is then obtained as

$$\left.\begin{aligned} \frac{dp}{dt}&=-(\beta\eta+v+\mu)p+\omega q+\kappa b+\text{higher order}+\text{nonlinear terms}\ldots \\ \frac{dq}{dt}&=vp-[(1-\varepsilon)\beta\eta+\omega+\mu]q+\text{higher order}+\text{nonlinear terms}\ldots \\ \frac{dr}{dt}&=\beta\eta p+(1-\varepsilon)\beta\eta q-(\sigma+\gamma_e+\mu)r+\text{higher order}+\text{nonlinear terms}\ldots \\ \frac{da}{dt}&=\sigma r-\left((\delta+\gamma_i+\mu)+\frac{\tau}{1+\alpha}\right)a+\text{higher order}+\text{nonlinear terms}\ldots \\ \frac{db}{dt}&=\gamma_i r+\left(\gamma_i+\frac{\tau}{1+\alpha}\right)a-(\kappa+\mu)b+\text{Higher order}+\text{nonlinear terms}\ldots \end{aligned}\right\} \quad (26)$$

Jacobian matrix of the system of (21),

$$\begin{vmatrix} -(\beta\eta+\nu+\mu) & \omega & 0 & 0 & \kappa \\ \nu & [(1-\varepsilon)\beta\eta+\omega+\mu] & 0 & 0 & 0 \\ \beta\eta & (1-\varepsilon)\beta\eta & -(\sigma+\gamma_e+\mu) & 0 & 0 \\ 0 & 0 & \sigma & -\left((\delta+\gamma_i+\mu)+\dfrac{\tau}{1+\alpha}\right) & 0 \\ 0 & 0 & \gamma_i & \left(\gamma_i+\dfrac{\tau}{1+\alpha}\right) & -(\kappa+\mu) \end{vmatrix} = 0 \quad (27)$$

The resulting eigenvalue of the above matrix is obtained as;

$$\left.\begin{aligned} &\left(-(\beta\eta+\nu+\mu)-\lambda_1\right)\left(-[(1-\varepsilon)\beta\eta+\omega+\mu]-\lambda_2\right)\left(-(\sigma+\gamma_e+\mu)-\lambda_3\right) \\ &\left(-\left((\delta+\gamma_i+\mu)+\frac{\tau}{1+\alpha}\right)-\lambda_4\right)(-(\kappa+\mu)-\lambda_5)=0 \end{aligned}\right\} \quad (28)$$

If

$$a=-(\beta\eta+\nu+\mu), b=-[(1-\varepsilon)\beta\eta+\omega+\mu], c=-(\sigma+\gamma_e+\mu), d=-\left((\delta+\gamma_i+\mu)+\frac{\tau}{1+\alpha}\right), e=-(\kappa+\mu)$$

it's therefore obtained that

$$\begin{aligned} &(a-\lambda_1)(b-\lambda_2)(c-\lambda_3)(d-\lambda_4)(d-\lambda_5)=0 \\ &\lambda^5-[(d+e)+(c+b)]\lambda^4+[(a+b)(c+d)+ab+cd]\lambda^3-[ab(c+d)+de(a+b)]\lambda^2 \\ &\quad +[ae+ad+bd+ac]+abcd=0 \end{aligned}$$

Hence, the persistent resilience of the model in a region are asymptotically stable.

2.8 Global Stability of Disease Free Equilibrium

Employing Lyapunov's function approach, we establish the global asymptotic stability of the proposed model for equation (1) at the Disease Free Equilibrium, utilizing the Lyapunov algorithm

$$\Phi(t,S,V,E,I,R)=C_1I_1+C_2I_2 \quad (29)$$

$$\frac{d\Phi}{dt}=C_1I_1^{\bullet}+C_2I_2^{\bullet}=C_1\left(\lambda S_0+(1-\varepsilon)\lambda V_0-(\sigma+\mu+\gamma_c)I_1\right)+C_2\left(\sigma I_1-(\gamma_i+\mu+\delta)I_2-\frac{\tau I_2}{1+\alpha I_2}\right)$$

$$\frac{d\Phi}{dt}\le C_1\left(\sigma+\lambda S_0+(1-\varepsilon)\lambda V_0-(\sigma+\mu+\gamma_c)\right)I_1-C_2\left((\gamma_i+\mu+\delta)+\frac{\tau}{1+\alpha}\right)I_2$$

$$\frac{d\Phi}{dt}\le C_1\left(\sigma+\left(\frac{\pi\beta\eta(1-\varepsilon)}{((1-\varepsilon)(\lambda+\nu+\mu)+\omega)}\right)^{-1}\frac{(\pi\beta\eta(1-\varepsilon))^2}{((\varepsilon-1)(\lambda+\nu+\mu)+\omega)}-(\sigma+\mu+\gamma_c)\right)I_1-C_2\left((\gamma_i+\mu+\delta)+\frac{\tau}{1+\alpha}\right)I_2$$

$$\frac{d\Phi}{dt}\le C_1\left(\sigma+\left(\frac{\pi\beta\eta(1-\varepsilon)}{((1-\varepsilon)(\lambda+\nu+\mu)+\omega)}\right)^{-1}\frac{(\pi\beta\eta(1-\varepsilon))^2}{((\varepsilon-1)(\lambda+\nu+\mu)+\omega)}-(\sigma+\mu+\gamma_c)\right)I_1-C_2\left(\left(\frac{(\gamma_i+\mu+\delta)(1+\alpha)}{\tau(\gamma_i+\mu+\delta)(1+\alpha)}\right)-\left(\frac{(\gamma_i+\mu+\delta)(1+\alpha)}{\tau(\gamma_i+\mu+\delta)(1+\alpha)}\right)\right)I_2$$

$$S_0 = \frac{\pi N(1-\varepsilon)}{\left((1-\varepsilon)(\lambda+\nu+\mu)+\omega\right)}, V_0 = \frac{\pi N}{\left((\varepsilon-1)(\lambda+\nu+\mu)+\omega\right)}, C_1 = \frac{(\sigma+\mu+\gamma_c)}{(\sigma+\mu+\gamma_c)}, C_2 = \left(\frac{(\gamma_i+\mu+\delta)(1+\alpha)}{\tau(\gamma_i+\mu+\delta)(1+\alpha)}\right)$$

$$\frac{d\Phi}{dt} \le C_1\left(\frac{\pi\tau(\alpha+1)(1-\varepsilon)+\sqrt{\pi\eta(1-\varepsilon)\beta+(\omega\kappa+\nu+\mu)}}{\left((1-\varepsilon)^2\alpha(\lambda+\nu+\mu)+\tau\omega\right)(\sigma+\gamma_e+\mu)(\delta+\gamma_i+\mu)} - \frac{(\sigma+\mu+\gamma_c)}{(\sigma+\mu+\gamma_c)}\right)I - C_2\left(\left(\frac{(\gamma_i+\mu+\delta)(1+\alpha)}{\tau(\gamma_i+\mu+\delta)(1+\alpha)}\right) - \left(\frac{(\gamma_i+\mu+\delta)(1+\alpha)}{\tau(\gamma_i+\mu+\delta)(1+\alpha)}\right)\right)$$

$$\frac{d\Phi}{dt} \le \psi(R_0-1)$$

It is pertinent to note that when at $t \to \infty$, $C_1 < 1 \text{and} \psi = \frac{\sigma}{(1-\varepsilon)}$. Substituting into the model system of equation (1) reveals that, based on LaSalle's invariance principle $\frac{d\Phi}{dt} = 0$, is globally asymptotically stable whenever $R_* < 1$

2.9 Sensitivity analysis of R_*

The primary aim is to assess the sensitivity of the basic reproduction number, by computing its derivative concerning all relevant parameters. This analysis will result in the determination of the normalized forward sensitivity index, denoted as

$$\begin{aligned}
&\frac{\partial R_0}{\partial \beta} = \frac{\partial R_0}{\partial \beta}\times\frac{\beta}{R_0} = 0.01206000, \frac{\partial R_0}{\partial \sigma} = \frac{\partial R_0}{\partial \sigma}\times\frac{\sigma}{R_0} = 1.03267370, \frac{\partial R_0}{\partial \alpha} = \frac{\partial R_0}{\partial \alpha}\times\frac{\alpha}{R_0} = 0.18743076\\
&\frac{\partial R_0}{\partial \mu} = \frac{\partial R_0}{\partial \mu}\times\frac{\mu}{R_0} = 0.15356728, \frac{\partial R_0}{\partial \kappa} = \frac{\partial R_0}{\partial \kappa}\times\frac{\kappa}{R_0} = 0.00001001, \frac{\partial R_0}{\partial \delta} = \frac{\partial R_0}{\partial \delta}\times\frac{\delta}{R_0} = 1.00000000\\
&\frac{\partial R_0}{\partial \gamma_e} = \frac{\partial R_0}{\partial \gamma}\times\frac{\gamma_e}{R_0} = 0.00000040, \frac{\partial R_0}{\partial \gamma_i} = \frac{\partial R_0}{\partial \gamma_i}\times\frac{\gamma_i}{R_0} = 0.00130200, \frac{\partial R_0}{\partial \varepsilon} = \frac{\partial R_0}{\partial \varepsilon}\times\frac{\varepsilon}{R_0} = 1.00200020\\
&\frac{\partial R_0}{\partial \tau} = \frac{\partial R_0}{\partial \tau}\times\frac{\tau}{R_0} = 1.00000000, \frac{\partial R_0}{\partial \omega} = \frac{\partial R_0}{\partial \omega}\times\frac{\omega}{R_0} = 1.000201001, \frac{\partial R_0}{\partial \pi} = \frac{\partial R_0}{\partial \pi}\times\frac{\pi}{R_0} = 1.00000014\\
&\frac{\partial R_0}{\partial \eta} = \frac{\partial R_0}{\partial \eta}\times\frac{\eta}{R_0} = 1.02030100,
\end{aligned} \tag{30}$$

Table 1. Sensitivity analysis and parameter indices

Parameters	Sensitivity indices
β	0.01206000
σ	1.03267370
α	0.18743076
κ	0.00001001
δ	1.00000000
ω	1.000201001

Table 1 shows that the values of the indices relative to basic reproduction number R_*, the sensitivity indices depend on the values of the other parameters, and changes in those values will affect the sensitivity indices. Based on the table, we can conclude that parameters are the most sensitive to the basic reproduction number in equation (1) of the meningitis model. Particularly, increasing the value of σ will result in a 96.96% increase in R_*, while increasing the value of ω will lead to a 91.52% decrease in R_*.

Table 2. Description of parameters, values, and references

Variable	Description		
S(t)	Susceptible population		
V(t)	Vaccinated population		
E(t)	Exposed population		
I(t)	Infected population		
R(t)	Recovered population		
Parameter	**Description**	**Values**	**References**
ε	Vaccination efficacy	0.002	[13]
ω	Vaccine waning rate	0.1	[8]
β	Transmission probability	1.0003	[17]
ν	Vaccination rate	0.5	[4]
η	Disease modification parameter	0.2	Assumed
γ_e	The recovery rate of exposed	0.03	[2]
γ_i	The recovery rate of infected	1.263	[20]
σ	Progression rate of exposure to infected	0.9	[26]
κ	Immunity waning rate	0.002	[9]
μ	Natural death	1.0	[5]
δ	Disease induced death	0.4	[7]
α	Saturated treatment inhibitor	0.008	[1]
τ	Treatment rate of infectious individual	1.82	Assumed
π	Recruitment rate	2.19	Assumed

3.0 Numerical simulation

To conduct numerical simulation on the mathematical model, we create the following correctional scheme for the model equation.

$$\left.\begin{aligned}
&(1-p)\frac{dS}{dt}+p\left(\frac{dS}{dt}-[\pi N+\omega V+\kappa R-\lambda S-(\nu+\mu)S]\right)=0\\
&(1-p)\frac{dV}{dt}+p\left(\frac{dV}{dt}-[\nu S-(1-\varepsilon)\lambda V-(\omega+\mu)V]\right)=0\\
&(1-p)\frac{dE}{dt}+p\left(\frac{dE}{dt}-[\lambda S+(1-\varepsilon)\lambda V-(\sigma+\mu+\gamma_c)E]\right)=0\\
&(1-p)\frac{dC}{dt}+p\left(\frac{dC}{dt}-[\sigma E-(\gamma_i+\mu+\delta)I-\frac{\tau I}{1+\alpha I}]\right)=0\\
&(1-p)\frac{dR}{dt}+p\left(\frac{dR}{dt}-[\gamma_c E+\left(\gamma_i+\frac{\tau I}{1+\alpha I}\right)I-(\kappa+\mu)R]\right)=0
\end{aligned}\right\} \quad (31)$$

The following correctional series are assumed as solutions for (1) such that

$$S(t)=\sum_{k=0}^{n}p^k s_k(t), V(t)=\sum_{k=0}^{n}p^k v_k(t), E(t)=\sum_{k=0}^{n}p^k e_k(t), I(t)=\sum_{k=0}^{n}p^k i_k(t), R(t)=\sum_{k=0}^{n}p^k r_k(t), \quad (32)$$

This series converges as p tends to 1.

Evaluating (27) and (28) and comparing coefficients of p^n yields the following

At $n = 0$

$$\frac{dS_o}{dt} = 0, \frac{dV_o}{dt} = 0, \frac{dE_o}{dt} = 0, \frac{dI_o}{dt} = 0, \frac{dR_o}{dt} = 0 \quad (29)$$

Solving these equations using the initial constraints

$$S_0(t) = s_0, V_0(t) = e_0, E_0(t) = e_0, I_0(t) = i_0, R_0(t) = r_0$$

Following this process yields

$$\begin{aligned} S_1(t) &= (\pi + \omega\nu + \kappa r_0 - \lambda s_0 - (\nu + \mu)s_0)t \\ V_1(t) &= (-\beta_1 s_0 - \beta_2 v_0 + \mu v_0)t \\ E_1(t) &= (\alpha s_0 i_0 - \mu e_0 - \sigma e_0)t \\ I_1(t) &= (\sigma e_0 - \mu i_0 - \delta i_0 - \rho i_0)t \\ R_1(t) &= (\rho i_0 - \mu r_0)t \end{aligned} \quad (33)$$

For $n = 2$

$$\begin{aligned} s_2(t) &= \frac{1}{2}t^2\begin{pmatrix} \alpha^3 i^2{}_0 s_0 + \alpha^2\mu i_0 s_0 + \alpha^2\beta_1 i_0 s_0 - \alpha^2\beta_2 i_0 v_0 - \alpha^2\theta i_0 + \alpha\delta i_0 s_0 + 2\alpha\mu i_0 s_0 + \alpha\rho_0 s_0 - \alpha\sigma e_0 s_0 + \alpha\beta_{10} s_0 + \mu^2 s_0 \\ + 2\mu\beta_1 s_0 - 2\mu\beta_1 v_0 - \beta_1{}^2 s_0 + \beta_2\beta_1 s_0 - \beta_2\beta_1 v_0 - \beta_2{}^2 v_0 - \mu\theta - \theta\beta_1 \end{pmatrix} \\ v_2(t) &= -\frac{1}{2}t^2\left(\alpha\beta_1 i_0 s_0 - \mu^2 v_0 + 2\mu\beta_1 s_0 - 2\mu\beta_2 v_0 + \beta_1{}^2 s_0 + \beta_2\beta_1 s_0 - \beta_2\beta_1 v_0 - \beta_2{}^2 v_0 - \theta\beta_1\right) \\ e_2(t) &= -\frac{1}{2}t^2\begin{pmatrix} \alpha^2 i_0{}^2 s_0 + \alpha\delta i_0 s_0 + 3\alpha\mu i_0 s_0 + \alpha\rho_0 s_0 - \alpha\sigma e_0 s_0 + \alpha\sigma_{10} s_0 + \alpha\beta_1 i_0 s_0 \\ - \alpha\beta_2 i_0 v_0 - \alpha\theta i_0 - \mu^2 e_0 - 2\mu\sigma e_0 - \sigma^2 e_0 \end{pmatrix} \\ i_2(t) &= -\frac{1}{2}t^2\left(\alpha\sigma i_0 s_0 + \delta^2 i_0 + 2\delta\mu i_0 + 2\delta\rho i_0 - \delta\sigma e_0 + \mu^2 i_0 + 2\mu\rho i_0 - 2\mu\sigma e_0 + \rho^2 i_0 - \rho\sigma e_0 - \sigma^2 e_0\right) \\ r_2(t) &= -\frac{1}{2}t^2\left(\delta\rho i_0 - \mu^2 r_0 + 2\mu\rho i_0 + \rho^2 i_0 - \rho\sigma e_0\right) \end{aligned} \quad (34)$$

For n = 3

$$S_3(t) = -\frac{1}{6}t^3\begin{pmatrix} \mu^3 s_0 + +2\mu\beta_1 s_0 - 2\mu\beta_2 v_0 + \beta_1{}^2 s_0 + \beta_2\beta_1 s_0 - \beta_2\beta_1 v_0 - \beta_2{}^2 v_0 \alpha^2\mu i_0 s_0 + \alpha^2\beta_1 i_0 s_0 - \alpha^2\beta_2 i_0 v_0 - \alpha^2\theta i_0 + \alpha\delta i_0 s_0 + \\ 2\alpha\mu i_0 s_0 + \alpha\rho_0 s_0 + 2\mu\beta_1 s_0 - 2\mu\beta_1 v_0 - \beta_1{}^2 s_0 + 5\beta_2\beta_1 s_0 - \beta_2\beta_1 v_0 - \beta_2{}^2 v_0 - \mu\theta - \theta\beta_1 - \alpha\sigma e_0 s_0 + \alpha\beta_{10} s_0 + \mu^2 s_0 + 3\mu\beta_1 s_0 \\ - 2\mu\beta_1 v_0 - \beta_1{}^2 s_0 + 4\beta_2\beta_1 s_0 + +2\mu\beta_1 s_0 - 2\mu\beta_1 v_0 - \beta_1{}^2 s_0 + \beta_2\beta_1 s_0 - 5\beta_2\beta_1 v_0 - 3\beta_2{}^2 v_0 - \alpha i_0 s_0 - \mu s_0 - 3\beta_1 s_0 + 2\beta_2 v_0 + \theta - \mu\theta - \theta\beta \\ {}_1 - 2\beta_2\beta_1 v_0 - \beta_2{}^2 v_0 - \mu\theta - \theta\beta - 5\beta_1 s_0 - \beta_2 v_0 + \mu v_0 - 3\mu\beta_1 s_0 - 2\mu\beta_2 v_0 + \beta_1{}^2 s_0 + \beta_2\beta_1 s_0 - \beta_2\beta_1 v_0 \_ + \delta^2 i_0 + 2\delta\mu i_0 + 2\delta\rho i_0 - \delta\sigma e_0 + \mu^2 i_0 \\ + 2\mu\rho i_{01} + 3\alpha\mu i_0 s_0 + \alpha\rho_0 s_0 - 3\alpha\sigma e_0 s_0 + \alpha\sigma_{10} s_0 + \alpha\beta_1 i_0 s_0 - \alpha\delta i_0 s_0 + 3\alpha\mu i_0 s_0 + \alpha\rho_0 s_0 - 2\alpha\sigma e_0 s_0 + \alpha\sigma_{10} s_0 \end{pmatrix}$$

$$v_3(t) = -\frac{1}{6}t^2\begin{pmatrix} \alpha\beta_1 i_0 s_0 - \mu^2 v_0 + 2\mu\beta_1 s_0 - 2\mu\beta_2 v_0 - -2\mu\beta_1 v_0 - \beta_1{}^2 s_0 + \beta_2\beta_1 s_0 - 5\beta_2\beta_1 v_0 - 3\beta_2{}^2 v_0 - \alpha i_0 s_0 - \mu s_0 - 3\beta_1 s_0 + 2\beta_2 v_0 + \theta - \mu\theta - \theta\beta \\ {}_1 - 2\beta_2\beta_1 v_0 - \beta_2{}^2 v_0 - \mu\theta - \theta\beta - 5\beta_1 s_0 - \beta_2 v_0 + \mu v_0 - 3\mu\beta_1 s_0 + \beta_1{}^2 s_0 + \beta_2\beta_1 s_0 - \beta_2\beta_1 v_0 - \beta_2{}^2 v_0 - \theta\beta_1 + + \alpha\delta i_0 s_0 + 3\alpha\mu i_0 s_0 + \alpha\rho_0 s_0 \\ - \alpha\sigma e_0 s_0 + \alpha\sigma_{10} s_0 - 2 + 2\mu\beta_1 s_0 - 2\mu\beta_2 v_0 + \beta_1{}^2 s_0 + 3\beta_2\beta_1 s_0 - \beta_2\beta_1 v_0 - \beta_2 v_0 + \mu v_0 - 3\mu\beta_1 s_0 - 2\mu\beta_2 v_0 + \beta_1{}^2 s_0 + \beta_2\beta_1 s_0 \end{pmatrix}$$

$$e_3(t) = -\frac{1}{6}t^2\begin{pmatrix} \alpha^2 i_0{}^2 s_0 + \alpha\delta i_0 s_0 + 3\alpha\mu i_0 s_0 + \alpha\rho_0 s_0 - \alpha\sigma e_0 s_0 + \alpha\sigma_{10} s_0 + \alpha\beta_1 i_0 s_0 + 2\mu\beta_1 s_0 - 2\mu\beta_1 v_0 - \beta_1{}^2 s_0 + 5\beta_2\beta_1 s_0 - \beta_2\beta_1 v_0 - \beta_2{}^2 v_0 - \mu\theta \\ - \alpha\beta_2 i_0 v_0 - 3\alpha\theta i_0 - \mu^2 e_0 - 2\mu\sigma e_0 - \sigma^2 e_0 - \mu^2 r_0 + 2\mu\rho i_0 + \rho^2 i_0 + \alpha\beta_1 i_0 s_0 - 4\alpha\delta i_0 s_0 + 3\alpha\mu i_0 s_0 + \alpha\rho_0 s_0 - 2\alpha\sigma e_0 s + + \alpha\delta i_0 s_0 + 3\alpha\mu i_0 s_0 + \alpha\rho_0 s_0 \\ - \alpha\sigma e_0 s_0 + \alpha\sigma_{10} s_0 + \alpha\beta_1 i_0 s_0 - \alpha\beta_2 i_0 v_0 - \alpha\theta i_0 - \mu^2 e_0 - 2\mu\sigma e_0 - \sigma^2 e_0 - \delta\rho i_0 - \mu^2 r_0 - 3\mu\beta_1 s_0 + \beta_1{}^2 s_0 + \beta_2\beta_1 s_0 - \beta_2\beta_1 v_0 - \beta_2{}^2 v_0 - \theta\beta_1 \\ + + \alpha\delta i_0 s_0 \sigma e_0 - \mu i_0 - \delta i_0 - \rho i_0 + 2\mu\rho i_0 - 2\mu\sigma e_0 + \rho^2 i_0 - \rho\sigma e_0 - \sigma^2 e_0 \end{pmatrix}$$

$$i_3(t) = -\frac{1}{6}t^2\begin{pmatrix} \alpha\sigma i_0 s_0 + \delta^2 i_0 + 2\delta\mu i_0 + 2\delta\rho i_0 - \delta\sigma e_0 + \mu^2 i_0 + 2\mu\rho i_0 - 2\mu\sigma e_0 + -\mu^2 r_0 + 2\mu\rho i_0 + \rho^2 i_0 + \alpha\beta_1 i_0 s_0 - 4\alpha\delta_0 s_0 + 3\alpha\mu i_0 s_0 + \alpha\rho_0 s_0 - 2\alpha\sigma e_0 s \\ + \alpha\delta_0 s_0 + 3\alpha\mu i_0 s_0 + \alpha\rho_0 s_0 - \alpha\sigma e_0 s_0 + \alpha\sigma_{10} s_0 + \rho^2 i_0 + -\beta_2{}^2 v_0 - \mu\theta - \theta\beta_1 - \alpha\sigma e_0 s_0 + \alpha\beta_{10} s_0 + \mu^2 s_0 + 3\mu\beta_1 s_0 - 2\mu\beta_1 v - \rho\sigma e_0 - \sigma^2 e_0 \\ + 2\mu\rho i_0 + \rho^2 i_0 + \alpha\beta_1 i_0 s_0 - 4\alpha\delta_0 s_0 + 3\alpha\mu i_0 s_0 + \alpha\rho_0 s_0 - 2\alpha\sigma e_0 s + + \alpha\delta_0 s_0 + 3\alpha\mu i_0 s_0 + \alpha\rho_0 s_0 \\ - \alpha\sigma e_0 s_0 + \alpha\sigma_{10} s_0 + \alpha\beta_1 i_0 s_0 - \alpha\beta_2 i_0 v_0 - \alpha\theta i_0 - \mu^2 e_0 - 2\mu\sigma e_0 - \sigma^2 e_0 - \delta\rho i_0 \end{pmatrix}$$

$$r_2(t) = -\frac{1}{6}t^2\begin{pmatrix} \delta\rho i_0 - \mu^2 r_0 + 2\mu\rho i_0 + \rho^2 i_0 + -\sigma^2 e_0 - \mu^2 r_0 + 2\mu\rho i_0 + \rho^2 i_0 + \alpha\beta_1 i_0 s_0 - 4\alpha\delta_0 s_0 + 3\alpha\mu i_0 s_0 + \alpha\rho_0 s_0 - 2\alpha\sigma e_0 s + + \alpha\delta_0 s_0 + 3\alpha\mu i_0 s_0 + \alpha\rho_0 s_0 \\ - \alpha\sigma e_0 s_0 + \alpha\sigma_{10} s_0 + \alpha\beta_1 i_0 s - \rho\sigma^2 e_0 \end{pmatrix}$$

This can be furthered till the desired number of iterations is obtained. Thus, the raw solutions to each model compartment are obtained as:

$$S(t) = \sum_{k=0}^{3} s_k(t), V(t) = \sum_{k=0}^{3} v_k(t), E(t) = \sum_{k=0}^{3} e_k(t), I(t) = \sum_{k=0}^{3} i_k(t), R(t) = \sum_{k=0}^{3} r_k(t), \tag{35}$$

And evaluating these results using the corresponding model parameters of each class given by

$$\left\{\begin{matrix} \alpha = 0.008, \delta = 0.4, \mu = 1.0, \omega = 0.1, \sigma = 0.9, \pi = 2.19, \gamma_1 = 1.263, \kappa = 0.002, \\ \gamma_e = 0.03, \tau = 1.82, v = 0.5, \eta = 0.2, \varepsilon = 0.002, \beta = 1.0003, e_0 = 65, s_0 = 500, i_0 = 23, v_0 = 120, r_0 = 14 \end{matrix}\right\}$$

We obtained that

$$\left.\begin{matrix} S(t) = 500 - 30.4320t + 0.7213561075t^2 - 0.03863404097t^3 \\ V(t) = 120 - 1.5060t - 0.01591470000t^2 + 0.00061794336453t^3 \\ E(t) = 65 + 18.1785t - 1.171778775t^2 + 0.04155466537t^3 \\ I(t) = 23 - 0.9060t + 0.02925067500t^2 - 0.0008440367800t^3 \\ R(t) = 14 - 0.0155t - 0.005054500000t^2 + 0.0001458242542t^3 \end{matrix}\right\} \tag{36}$$

The approximate results of each class are evaluated using their respective baseline values in Table 1. We also suggest the following population data set as initial values given by $s_0 = 1000,\ e_0 = 30,\ i_0 = 20,\ r_0 = 40$. Thus we obtain the following series of results embedding the parameters whose influence on the dynamics of meningitis transmission are to be analyzed

$$s(t) = 1000 + \begin{pmatrix} 65.26869000 + 1.3362000\alpha \\ -1362.924000\alpha^2 - 37.68c \end{pmatrix}t + \begin{pmatrix} -8.99856418\alpha^2 \\ +5499.838828\alpha^4 \\ 54.0914019 \\ +152.0510083\alpha^2 c \\ -0.09970881600\alpha c \\ +3333.926349 \\ 45.98509816c \\ -3.288025569\alpha \end{pmatrix}\frac{t^2}{2} - \begin{pmatrix} 11.30828286\alpha^2 c^2 \\ -66.76103861\alpha^3 \\ -0.003719829888\alpha c^2 \\ +40645.08576\alpha^4 \\ +935.98111186\alpha^2 c \\ +56.12092345c \\ -5.923814565\alpha \\ 302.0838612 \\ +36988.74452\alpha^6 \\ -84.74264814\alpha \end{pmatrix}\frac{t^3}{6}$$

$$e(t) = 30 + \begin{pmatrix} -45.62599000 \\ +1362.924999\alpha^2 \\ -1.336200000\alpha \end{pmatrix} t - \begin{pmatrix} -69.38980854 \\ -8.998569418\alpha^3 \\ +5499.839928\alpha^4 \\ +152.0510083\alpha^2 c \\ -0.09970881600\alpha c \\ +5378.993811\alpha^2 \\ +0.0000493608c \\ -5.292993669\alpha \end{pmatrix} \frac{t^2}{2} + \begin{pmatrix} 11.30828286\alpha^{2^2} - 80.26339203\alpha^3 \\ -105.5276927 - 0.003719829888\alpha c \\ +48897.59557\alpha^4 + 1164.133657\alpha^2 c \\ -0.7679873978\alpha c + 1431.639314\alpha^4 c \\ -1.875838588\alpha^3 c + 16753.17626\alpha^2 \\ +0.0003841080404c - 16.31203298\alpha \\ +36988.74452\alpha^6 - 84.74264814\alpha^5 \end{pmatrix} \frac{t^3}{6}$$

$$i(t) = 20 - 50.40320t - \begin{pmatrix} 127.0391180 \\ +0.681642000\alpha^2 \\ -0.000668100\alpha \end{pmatrix} \frac{t^2}{2} - \begin{pmatrix} -0.004499284709\alpha^3 \\ +320.2194878 \\ +2.749919964\alpha^4 \\ +0.07602550416\alpha^2 c \\ -0.00004985440800\alpha c \\ +4.407401276\alpha^2 \\ +2.468040000 \cdot 10^{-8} c \\ -0.004330716805\alpha \end{pmatrix} \frac{t^3}{6}$$

$$r(t) = 40 + (46.18360 + 37.68c)t - \begin{pmatrix} 250.8099123 \\ +45.9850488c \\ -2044.386000\alpha^2 \\ +2.004300000\alpha \end{pmatrix} \frac{t^2}{2} + \begin{pmatrix} 13.49785413\alpha^3 \\ -8249.759899\alpha^4 \\ +727.7734324 \\ -228.0765125\alpha^2 c \\ +0.1495632240\alpha c \\ -10561.77617\alpha^2 \\ +56.12053936c \\ +10.38388802\alpha \end{pmatrix} \frac{t^3}{6}$$

Results and discussion

Pictorial interpretation of numerical simulation

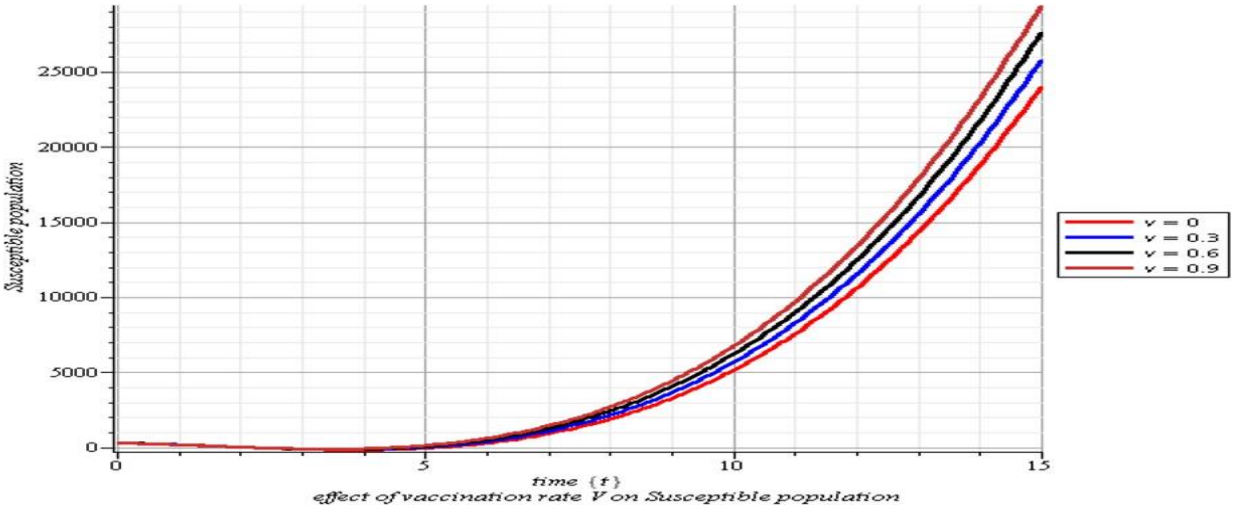

Fig 2. Effect of vaccination rate v on susceptible population

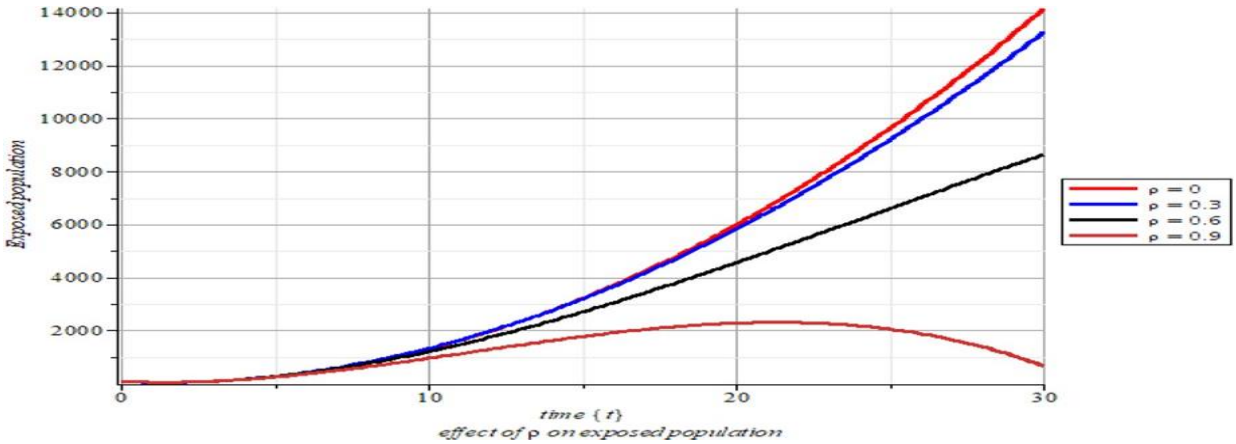

Fig.3. Effect of vaccination rate v on exposed population

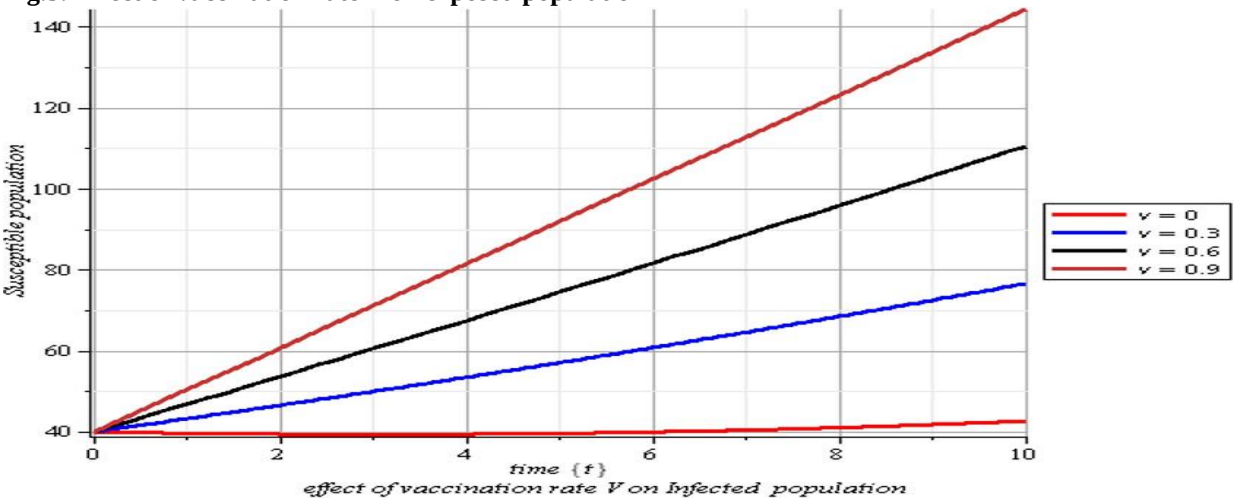

Fig. 4. Effect of vaccination rate on infected population

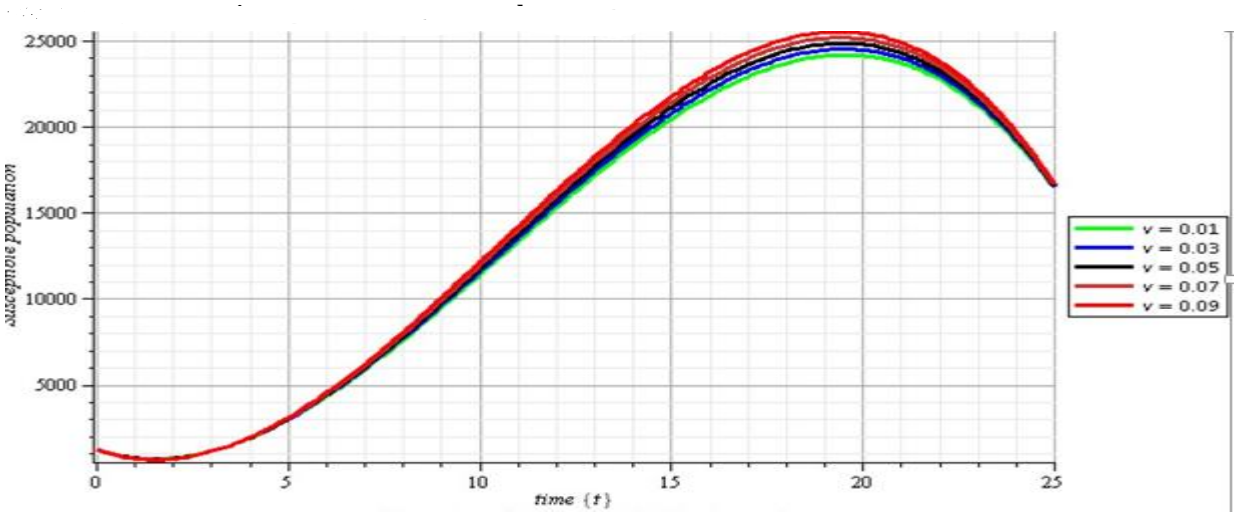

Fig. 5. Effect of vaccination rate ω on infected population

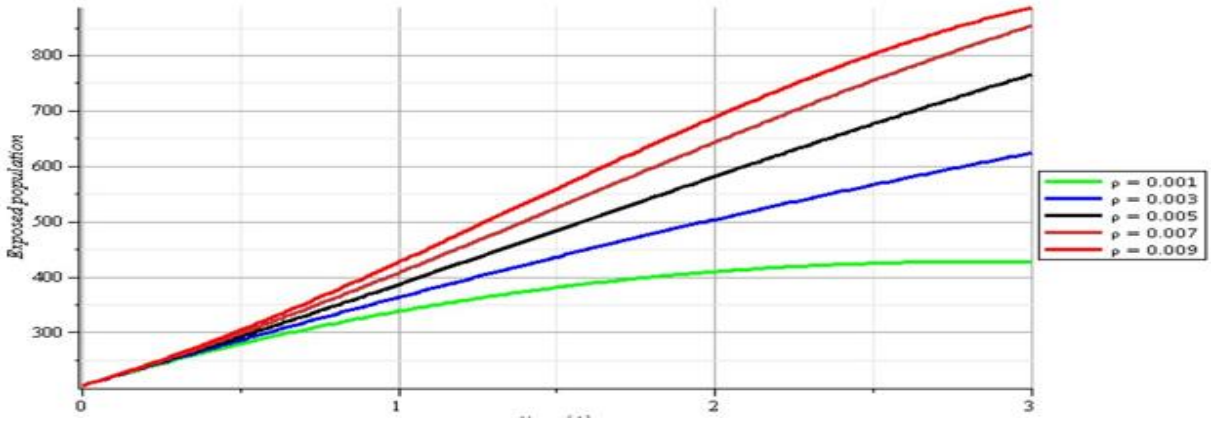

Fig. 6. Effect of vaccination rate ω on susceptible population

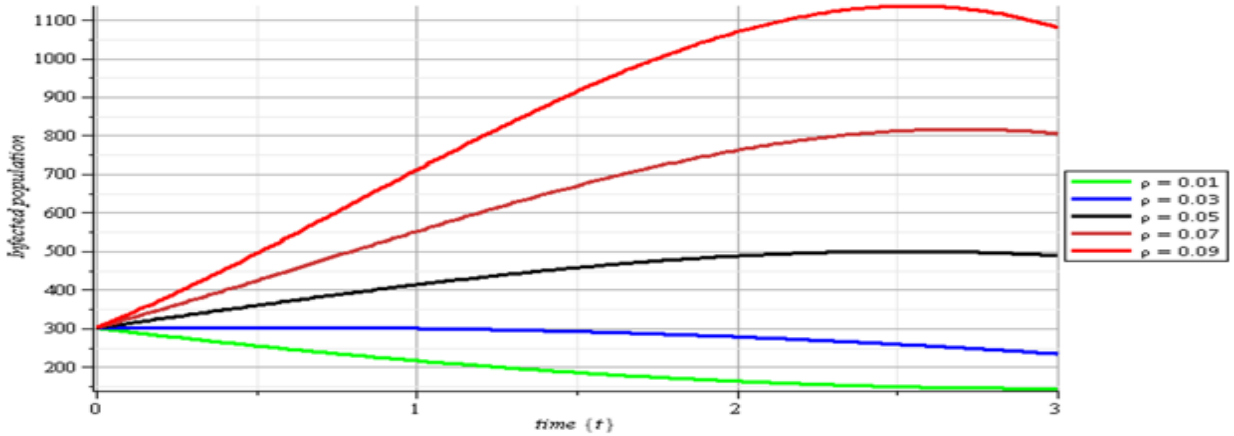

Fig. 7. Effect of vaccination rate ω on exposed population

Discussion

Was utilized to simulate the disease dynamics over time. The findings are presented in a graphical format and extensively discussed. Fig.2 illustrates that as the vaccination rate increases, the vulnerable population also increases. Meanwhile, fig. 3 demonstrates that when the vaccination rate goes from 0.0 to 0.9, the exposed population decreases. This suggests that an increase in vaccination rates results in a higher number

of susceptible individuals and a decrease in vaccination rates leads to a higher number of exposed individuals. Additionally, as the vaccination rate rises, the exposed population decreases, as observed in fig 4. Over a period of 20 months, it was noted that as the vaccination rate increases from 0.03 to 0.09, the infected population decreases.

Fig 5 reveals that an increase in vaccination results in a reduction in the number of infected individuals, consequently increasing the population of susceptible individuals. Fig. 6 highlights the impact of vaccination on the susceptible population, particularly after recovery. Through treatment, susceptible individuals can be effectively recovered from the disease. In this context, vaccinating those who have recovered can significantly reduce the prevalence of the disease in the population. Fig. 7 explores the effects of the waning rate on exposed individuals. An increase in the waning rate leads to a reduction in the population of exposed individuals. For instance, when the waning rate is 0.01, more individuals are less likely to become infected, resulting in an increased population of susceptible individuals. Conversely, reducing the waning rate increases the infected population.

Conclusion

The study aimed to utilize the homotopy perturbation method to derive a numerical solution for the impact of high treatment vaccination efficacy on a meningitis model of SVEIR. This simulates the effects of treatment and vaccination on an individual's in the sub-population considered and its effects based on target parameter values from the model formulation yielding to an effectively accurate model results. Subsequently, numerical output was simulated to assess the influence of vaccination saturation on meningitis transmission within the population, with careful analysis of the accompanying graphs to reveal key experimental findings as in [12, 17, 28 and 33]. Nevertheless, it is important to note that further research is essential to address the ongoing prevalence of this epidemic disease and to develop effective strategies for its containment and eradication. The promotion of awareness and preventive measures is crucial for controlling the spread of meningitis in the future.

Financial support
TETFund BRE

Declaration of Competing Interest
The authors of the paper declared that there are no conflicts of interest.

5. ACKNOWLEDGMENT

Authors acknowledged tremendous efforts and financial grant from Tertiary Education Trust Fund (TETFund).

References

[1] Bell W. E, McCormick WF (2019). Neurologic infections in children. 2nd ed. Vol. 12 of Major problems in clinical pediatrics. Philadelphia: W.B. Saunders, 77-80.

[2] Naraqi S, Kirkpatrick GP, Kabins S (2020). Relapsing pneumococcal meningitis: isolation of an organism with decreased susceptibility to penicillin G. J Pediatr; Vol 85:671-3.

[3] Mutairu K. Kolawole, Kazeem, A. Odeyemi , Asimiyu O. Oladapo and Kehinde A. Bashiru (2022) Dynamical Analysis and Control Strategies for Capturing the Spread of Covid-19. Tanzania Journal of Science 48(3): 680-690.

[4] Mutairu k. Kolawole, Oluwarotimi O. Aderonke, Kazeem, A. Odeyemi, Amos O. Popoola (2023) Analysis of Corona-Virus Mathematical Model in Asymptotic and Symptomatic Cases with Vaccine using Homotopy Perturbation Method. Journal of Applied Computer Science & Mathematics, Issue 1, vol.17, No. 35.

[5] Friedland IR, Shelton S, Paris M (2021), Dilemmas in diagnosis and management of cephalosporin-resistant Streptococcus pneumoniae meningitis. Pediatr Infect Dis; 12:196-200.

[6] Mustafa MM, Ramilo O, Mertsola J (2022), Modulation of inflammation and cachectic activity in relation to treatment of experimental Haemophilus influenzae type b meningitis. J Infect Dis; 160:818-25.

[7] Radetsky M (2023). Duration of symptoms and outcome in bacterial meningitis: an analysis of causation and the implications of a delay in diagnosis. Pediatr Infect Dis J; 11:694-8.

[8] Schaad UB, Suter S, Gianella-Borradori A (2020), A comparison of ceftriaxone and cefuroxime for the treatment of bacterial meningitis in children. N Engl J Med; 322:141-7.

[9] Mutairu k. Kolawole, Kazeem, A. Odeyemi, Kehinde A. Bashiru, Amos O. Popoola (2023) An Approximate Solution of Fractional Order Epidemic Model of Typhoid using Homotopy

Perturbation Method. Uniosun Journal of Engineering and Environmental Sciences, Vol. 5 No. 1. DOI: 10.36108/ujees/3202.50.0180.

[10] Mutairu K. Kolawole, Morufu O. Olayiwola, Kazeem, A. Odeyemi, (2023) Extensive Analysis and Projection of the Impact of High-Risk Immunity Using a Mathematical Model That Incorporate a Convex Incidence Rate of Multiple Covid-19 Exposures. Cankaya University Journal Science and Engineering. CUJSE 20(02): 107-128.

[11] Talan DA, Zibulewsky J (2020). Relationship of clinical presentation to time to antibiotics for the emergency department management of suspected bacterial meningitis. Ann Emerg Med; 22:1733-8.

[12] Coant PN, Kornberg AE, Duffy LC, Dryja DM, Hassan SM (2023). Blood culture results as determinants in the organism identification of bacterial meningitis. Pediatr Emerg Care; 8:200-5

[13] Quagliarello V, Scheld WM (2020). Bacterial meningitis: pathogenesis, pathophysiology, and progress. N Engl J Med; 327:864-72

[14] Wald ER, Kaplan SI, Mason EO Jr (2017), Dexamethasone therapy for children with bacterial meningitis. Pediatrics 1995; 95:21-8.

[15] Mutairu K. Kolawole, Muideen O. Ogunniran, Kazeem, A. Odeyemi (2023) On the Numerical Simulation of the Effect of Disease Transmission Coefficient on SEIR Epidemic Model Using Hybrid Block Method. Jurnal diferensial. Issue 2, Vol 5 No. 2. DOI: https://doi.org/10.35508/jd.v5i2. Indonesia

[16] W.H.O (World Health Organization) (2020) Emergencies, preparedness, response. Pneumonia of unknown origin-China, Disease Outbreak News. 5. https:// www. Who. int/ csr/ don/ 05- janua ry- 2020- pneum onia- of-unknown ncause- china/ en/. Accessed 5 Mar 2020

[17] Kanra GY, Ozen H, Secmeer G, Ceyhan M, Ecevit Z, Belgin E (2019). Beneficial effects of dexamethasone in children with pneumococcal meningitis. Pediatr Infect Dis J; 14:490-4.

[18] M. K. Kolawole, M. O. Ogunniran, and K. R. Tijani, "Simulating the effect of disease transmission coefficient on a disease induced death series epidemic model using the homotopy perturbation method," Journal of Applied Computer Science & Mathematics, vol. 16, no. 33, 2022.

[19] Mutairu K. Kolawole, Bukola. O. Akin-awoniran, Kazeem, A. Odeyemi (2023) On the Numerical Analysis of the Effect of Vaccine on Measles using Virational Iteration Method. Jurnal diferensial. Issue 2, Vol 5 No. 2. DOI: https://doi.org/10.35508/jd.v5i2.

[20] Girgis NI, Farid Z, Mikhail IA, Farrag I, Sultan Y, Kilpatrick ME (2019). Dexamethasone treatment for bacterial meningitis in children and adults. Pediatr Infect Dis J; 8:848-51.

[21] Lebel MH, Freij BJ, Syrogiannopoulos GA (2023), Dexamethasone therapy for bacterial meningitis: results of two double-blind, placebo-controlled trials. N Engl J Med; 319:964-71

[22] Sáez-Llorens X, Ramilo O, Mustafa MM (2022), et al. Molecular pathophysiology of bacterial meningitis: current concepts and therapeutic implications. J Pediatr; 116: 671–84.

[23] Leib SL, Tauber MG (2018). Pathogenesis of bacterial meningitis. Infect Dis Clin North Am; 13: 527–48.

[24] Braun JS, Tuomanen EI (2024). Molecular mechanisms of brain damage in bacterial meningitis. Adv Pediatr Infect Dis; 14: 49–71.

[25] Peltola H. Worldwide H influenzae type b disease at the beginning of the 21st century: global analysis of the disease burden 25 years after the use of the polysaccharide vaccine and a decade after the advent of conjugates. Clin Microbial Rev 2000; 13: 302–17

[26] Rodriguez AF, Kaplan SL, Mason EO Jr (2020). Cerebrospinal fluid values in the very low birth weight infant. J Pediatr; 116: 971–74.

[27] Augusto and M. Leite, "Optimal control and cost-effective analysisofthe2017meningitisoutbreakinNigeria, " Infectious Disease Modelling, vol. 4, pp. 161–187, 2019.

[28] F. Dejongh, "New global meningitis strategy aims to save 200,000 lives a year," 2021, https://news.un.org/en/story/ 2021/09/1101352.

[29] N. K.-D. O. Opoku and C. Afriyie, "The role of control measures and the environment in the transmission dynamics of cholera," Abstract and Applied Analysis, vol. 2020, Article ID 2485979, 16 pages, 2020.

[30] J. K. K. Asamoah, F. Nyabadza, B. Seidu, M. Chand, and H. Dutta, "Mathematical modeling of bacterial meningitis transmission dynamics with control measures," Computational and Mathematical Methods in Medicine, vol. 2018, Article ID 2657461, 21 pages, 2018.

[31] I. M. EL Mojtaba and S. O. Adam, "A mathematical model for meningitis disease," Red Sea University Journal of Basic and Applied Science, vol. 2, no. 2, pp. 467–472, 2017

[32] Ayoola T, Kolawole M, Popoola A (2022) "Mathematical Model of COVID-19 Transmission Dynamics with Double Dose Vaccination". https://www.ajol.info/index.php/tjs

[31] Waage A, Halstensen A, Espevik T (2021). Association between tumor necrosis factor in serum and fatal outcome in patients with meningococcal disease. Lancet; 1: 355–57.

[32] Feldman WE (2017). Relation of concentrations of bacteria and bacterial antigen in cerebrospinal fluid to prognosis in patients with bacterial meningitis. N Engl J Med; 296: 433–35.

[33] Converse GM, Gwaltney JM Jr, Strassburg DA, (2023). Alteration of cerebrospinal fluid findings by partial treatment of bacterial meningitis. J Pediatr; 83: 220–25.

[34] Koedel U, Scheld WM, Fister H. W (2022). Pathogenesis and pathophysiology of pneumococcal meningitis. Lancet Infect Dis; 2: 721–36.

[35] Margall Coscojuela N, Majo Moreno M, Latorre Otin C, Fontanals Amyerich D, Dominguez Garcia A, Prats Pastor G (2023). Use of universal PCR on cerebrospinal fluid to diagnose bacterial meningitis in culture-negative patients. Eur J Clin Microbiol Infect Dis; 21: 67–69.

[36] Pollard AJ, Probe G, Trombley C, (2021). Evaluation of a diagnostic polymerase chain reaction assay for Neisseria meningitidis in North America and field experience during an outbreak. Arch Pathol Lab Med; 126: 1209–15.

[37] Feldman WE (2017). Concentrations of bacteria in cerebrospinal fluid of patients with bacterial meningitis. J Pediatr; 88: 549–52.

[38] Portnoy JM, Olsen LC (2018). Normal cerebrospinal fluid values in children: another look. Pediatrics; 75: 484–87.

[39] Saravolatz LD, Manzor O, VanderVelde N, Pawlak J, Belian B (2020). Broad-range bacterial polymerase chain reaction for early detection of bacterial meningitis. Clin Infect Dis. Vol 4(1) 244-268

[40] Leib SL, Leppert D, Clements J, Tauber MG (2016). Matrix metalloproteinase contribute to brain damage in experimental pneumococcal meningitis. Infect Immune; 68: 615–20.

[41] Tuomanen E (2015). Molecular mechanisms of inflammation in experimental pneumococcal meningitis. Pediatr Infect Dis; 6: 1146–49.